An investigation of the crack propagation in tool steel X38CrMoV5(AISI H11) in SET specimens

Masood Shah, Catherine Mabru, Christine Boher, Sabine Le Roux, Farhad Rezai-Aria

An investigation of the crack propagation in tool steel X38CrMoV5 (AISI H11) in SET specimens

MASOOD SHAH[a], CATHERINE MABRU[b], CHRISTINE BOHER[a], SABINE LEROUX[a], FARHAD REZAI-ARIA[a]

[a] Laboratoire Centre de Recherche, Outillages, Matériaux et Procédés (CROMeP), Université Toulouse Ecole Mines Albi, France
[b] Département Mécanique des Structures et Matériaux (DMSM), d'Institut Supérieur de l'Aéronautique et de l'Espace (ISAE), Toulouse, France

Abstract An approach is proposed for the evaluation of surface fatigue damage of hot forming tools that undergo severe thermo mechanical loading. Fatigue crack propagation in a hot work tool steel X38CrMoV5-47HRC is investigated using single-edge cracked tension specimens with 3 different thicknesses (2.5, 1, 0.6 mm) and two R-values.

The stress intensity factor is evaluated with ABAQUS®. Paris curves are established for the crack propagation experiments.

1 INTRODUCTION

An approach for the study of sub-surface damage experienced in machining, tool wear, hot forming tools is proposed. For example, studies on pressure die casting dies [1,2] show that the surface damage in tool steels extends from the surface down to 50-300 µm into the bulk material (this thickness will hereafter be referred to as the "surface"). It is also known that the properties of materials of low thickness may be different from those of bulk materials [3-5]. It is thus proposed to study the crack initiation and propagation behaviour of the surface separately from the bulk Figure 1. Initial results in testing procedure are presented.

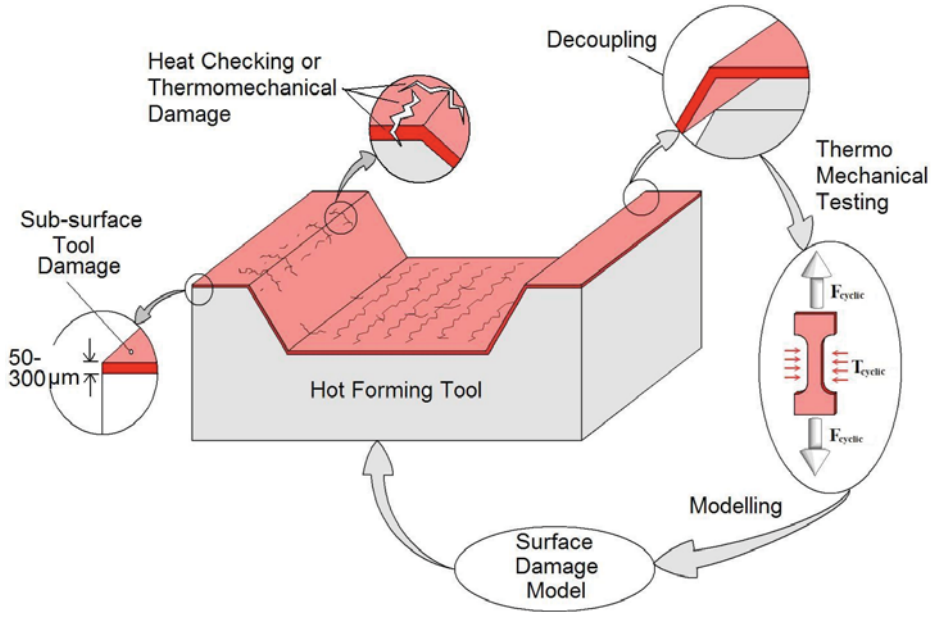

Figure 1. General procedure for the study of surface damage in tool steels.

2 MATERIAL AND SPECIMEN PREPARATION

Material

The experiments are carried out on a hot work martensitic tool steel X38CrMoV5 (AISI H11) delivered free of charge by AUBERT & DUVAL in the form of forged bars of 60 mm square section. It is a low Si and low NMP content, 5% Chrome steel principally used in HPDC industry. The steel is quenched and double tempered to a hardness of 47 HRC and σ_y of 1000 MPa. The chemical composition by weight % is given in Table I.

Table I. Chemical composition of tested steel (%weight)

Elements	C	Cr	Mn	V	Ni	Mo	Si	Fe
% Mass	0.36	5.06	0.36	0.49	0.06	1.25	0.35	bal

Specimen Preparation and Test

All SET specimens are machined by wire cut electro erosion on a AGIECUT 100D wire cut machine Figure 2a. The flat surfaces of the specimens are then ground parallel on an LIP 515 surface grinder. As a last stage specimens are polished on a metallographic polisher BUEHLER® PHEONIX 4000, to obtain a mirror finish with a 1 micrometer grit diamond paste. A grid of 0.10*0.10mm is marked on the polished surfaces Figure 2b.

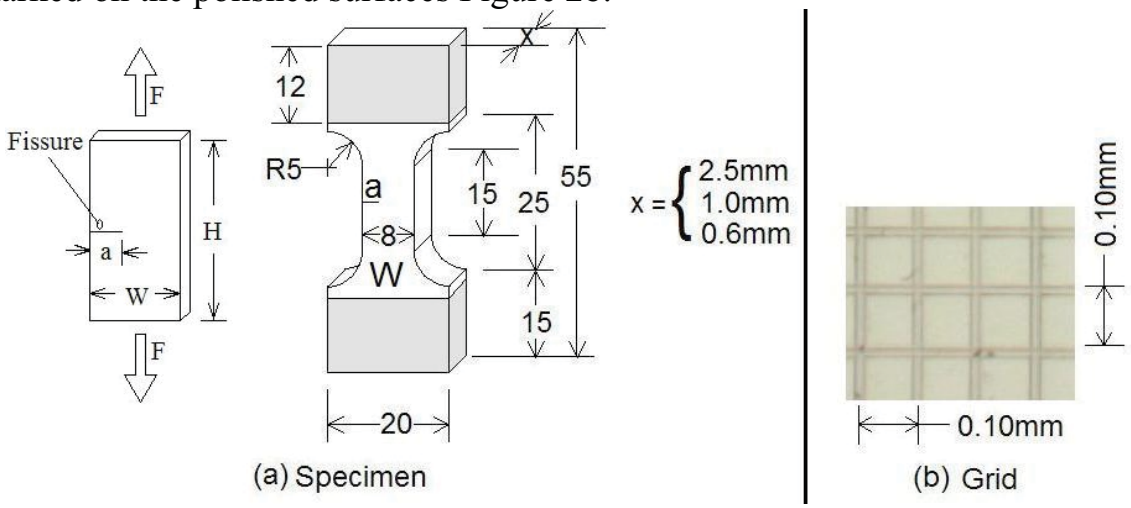

Figure 2. Specimen geometry and engraved grid on specimen surface.

The crack propagation experiments were carried out on a servo hydraulic universal testing machine WALTER + BAI LFV 40 at an ambient temperature of 25°C. Propagation is optically observed in situ with a QUESTAR® observation microscope (0.0012 mm resolution) without interruptions. Three different thicknesses 2.5mm, 1.0mm, 0.6mm were tested to evaluate the effects of thickness on the crack propagation behaviour at room temperature.

3 NUMERICAL SIMULATION

One of the main concerns in a crack propagation experiment on SET specimens is the accurate evaluation of the stress intensity factor K_I. ABAQUS® calculates the J-Integral for different values of a/W, which are used to evaluate K_I using the equation (1). An expression for correction factor F(a/W) is then established by

using equation (2). “E” represents the young’s modulus, “σ” applied stress, “a” crack length and “W” width of specimen.

$$K_I = \sqrt{J \times E\left(1/1-\upsilon^2\right)} \tag{1}$$

$$K_I = F\left(\frac{a}{W}\right).\sigma\sqrt{\pi a} \tag{2}$$

Verification of the K_I Calculation Procedure

The correction factor F(a/W) is strongly dependent on the value of H/W. The form of the specimen being used lies between H/W=2 and H/W=3. Finite element analyses are initially carried out on standard SET specimens of H/W=2 Figure 3a and H/W=3 Figure 3b for range, $0.125 \leq a/W \leq 0.625$ with equal steps of 0.125. These values are then compared with those calculated by Chiodo et al. [6,7] and John et al. [8] Figure 4a.

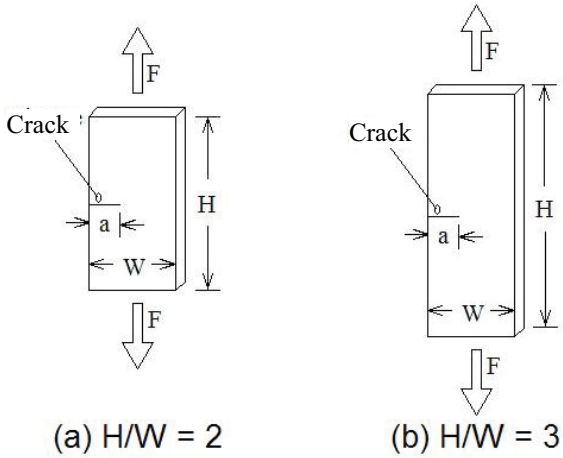

Figure 3. Schematic of the SET standard specimens.

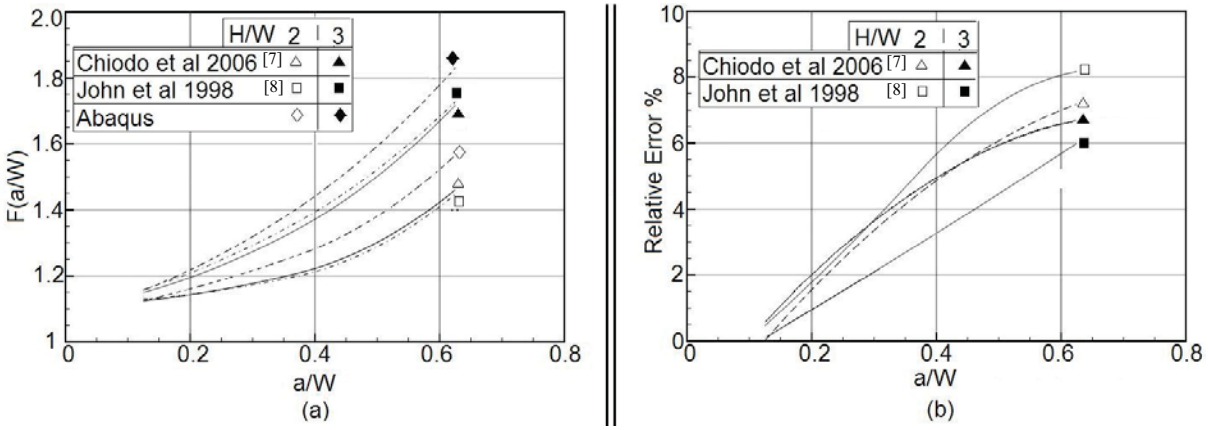

Figure 4. (a) Variation of correction factor F(a/W) vs. a/W at two H/W ratios. (b) Relative error of F(a/W) estimation between ABAQUS® and [7] and [8]

The relative error is defined as: $(F_c\text{-}F_l)/F_l$, where F_c = calculated correction factor using ABAQUS® and F_l = correction factor from literature. This error in Figure 4b does not exceed 8% over the whole range of crack measurement. There is also a tendency towards stabilisation of the error with increasing a/W. It was therefore considered that the procedure of evaluation of K_I with ABAQUS® is relevant for the test conditions presented here.

An expression is thus obtained of F(a/W) for the specimen in Figure 2a.

$$F\left(a/W\right) = 1.1188 - 0.0412\left(a/W\right) + 3.2155\left(a/W\right)^2 - 4.7872\left(a/W\right)^3 + 3.9253\left(a/W\right)^4 \quad (3)$$

Equation (3) is used in conjunction with equation (2) to calculate K_I.

Calculation Procedure of K_I using ABAQUS® J-Integral

This procedure is schematically shown in Figure 5. First, in order to define a crack, a plane partition is defined on one edge of the SET specimen, which is lengthwise centred. The edge of the plane inside the specimen defines the crack front Figure 5-1. A region of sufficient volume is isolated around the partition. This region is fine meshed as compared to the other regions of the specimen which serves to reduce the simulation time Figure 5-2.

Next, a cylindrical region is isolated at the crack tip Figure 5-3. Wedge elements of type C3D15 (3D Stress wedge elements) shown in Figure 6a are used to create the required crack tip singularity. Lastly, a larger cylinder around the crack tip is isolated and meshed using C3D20R (3D Stress, 20 node quadratic brick elements, reduced integration) elements Figure 6(b). This cylinder is used for creating the contour paths necessary to evaluate the contour integral or J values. Five contours are created around the crack front to have an effective evaluation of the plain strain K_I.

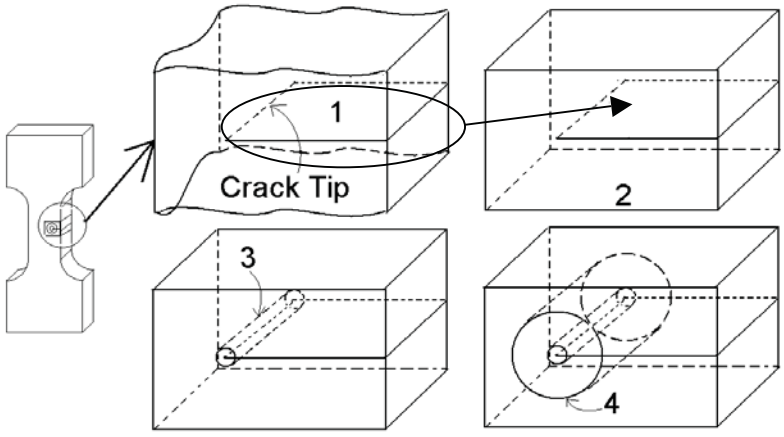

Figure 5. Crack Modelling Procedure

Fifteen layers of elements are meshed in the within the thickness of the specimens. The value of J-Integral thus calculated depends on the distance of the elements from the free surfaces. An average of all values of J calculated at different depths from the free surface is taken. This average value of J is then used with equation 1 and 2 to calculate K_I and F(a/W).

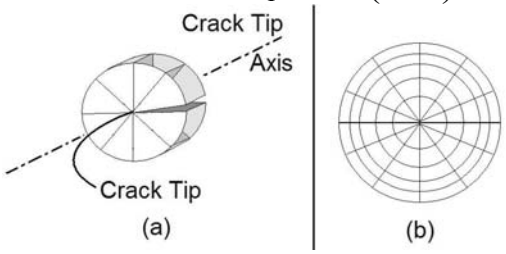

Figure 6. (a) Wedge elements at the crack tip, (b) Contour integral meshing.

4 FATIGUE PROPAGATION AND RESULTS

The test specimens of thickness 2.5mm have been tested at two different stress ratios of R=0.1 and 0.7 for crack propagation, while those of thicknesses 1.0mm and 0.6mm have been tested only at R = 0.1. Following the experiments, the Paris curves for all the specimens have been established using $\Delta a/\Delta N$. These curves have then been compared with each other to study the effects of variability of R and of the specimen thickness. The test conditions are summarized in Table II.

Table II. Conditions for Crack Propagation Experiments

Thickness (mm)	Applied stress / Yield stress (%)	Stress ratio $R=\sigma_{min}/\sigma_{max}$	Test Frequencies (Hz)
2.5	25 / 8.3	0.1	10
2.5	25	0.7	
1.0		0.1	
0.6		0.1	

One characteristic curve for R=0.7 is presented in Figure 7. The different values of constants m and C of the Paris law [9] (equation 4.), determined for all the experiments are summarized in Table III.

$$\Delta a/\Delta N = C.\Delta K^m \tag{4}$$

The slope of the propagation curves tends to increase approaching threshold ΔK_I. However due to large dispersion in data the threshold values could not be clearly identified.

Table III. Paris law constants

N°	e mm	R	m	C
1	2.5	0.1	2.39	0.72e-10
2	2.5	0.1	2.08	1.43e-10
3	2.5	0.7	2.04	2.62e-10
4	2.5	0.7	2.32	1.06e-10
5	0.6	0.1	2.18	1.07e-10

In the Figure 8 a comparison is provided between R = 0.1 and 0.7 crack propagation rates. It is evident that the crack propagation rates tend to increase with ascending R. Also compared are the propagation curves for different thicknesses (Figure 9) 2.5 and 0.6 mm at R=0.1. It can be seen that the data has a tendency to slide rightwards i.e., reduced values of crack propagation rate for the same ΔK_I.

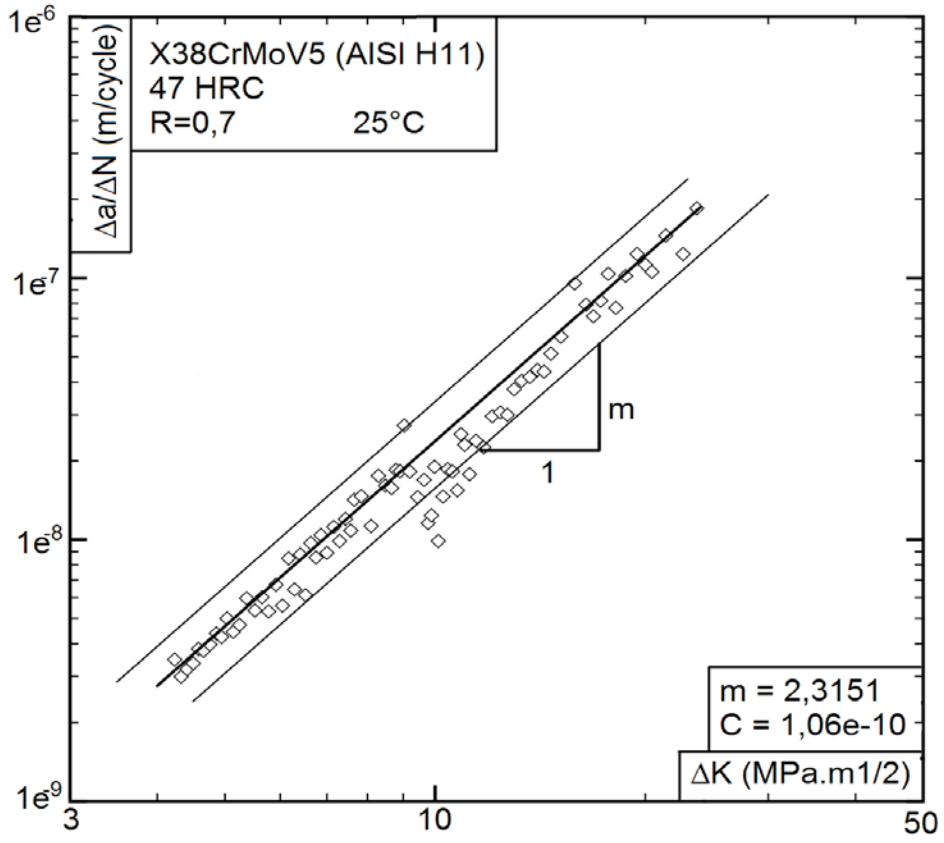

Figure 7. Example of Paris curve for R=0.7

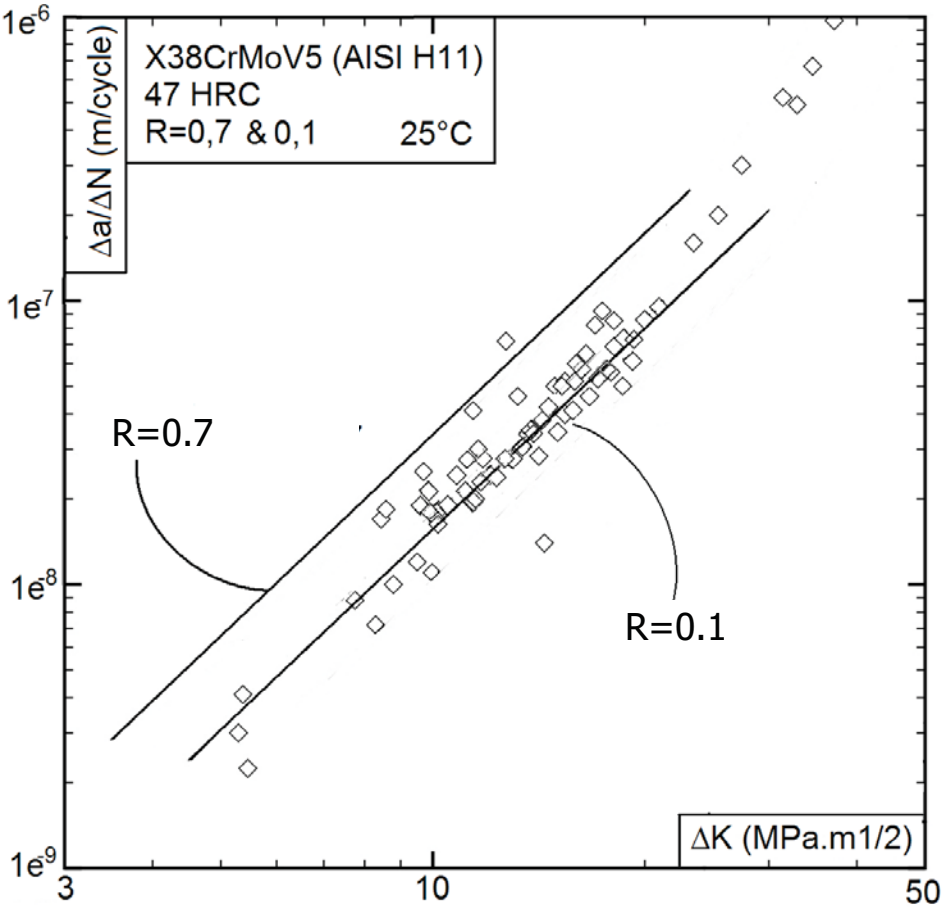

Figure 8. Comparison of Paris curves for R=0.7 and 0.1

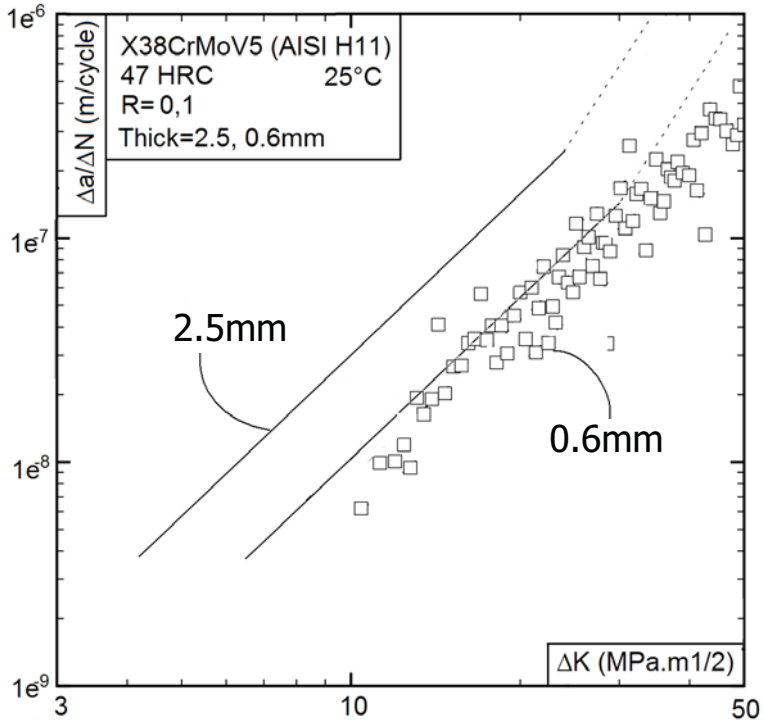

Figure 9. Comparison of Paris curves for thickness 2.5mm and 0.6mm at R=0.1

5 DISCUSSION

At 0.6mm it seems that the testing condition approaches plane stress condition. Detailed optical observations have also revealed an important crack tip plastic zone. In the 0.6mm thickness specimen, formation of patterns related to plastic deformation was also observed on the surface, which has not previously been observed on LCF experiments on this material [10, 11] on solid cylindrical specimens. An effort was also made to measure the crack tip opening displacement and crack closure in situ by optical measurements. At this stage no clear crack closure could be demonstrated.

The difference in the crack propagation curves may be explained by two reasons. First the K_I, have been calculated for plane strain condition with small scale yielding. In the experiments, these conditions do not strictly prevail. In particular in the 0.6mm specimen the effect of the plane stress and large plastic zone has to be considered. The second explanation could be a different crack closure mechanism due to larger plastic deformations at the crack tip of the 0.6mm specimen compared to the 2.5mm specimen. More work has to be done on the stress state of the crack tip to have better insight into the difference in crack propagation curves.

6 CONCLUSION

Crack propagation experiments have been performed on SET specimens made of a hot work martensitic tool steel X38CrMoV5 (AISI H11). The effect of loading ratio R is studied. It is seen that the crack propagation rate increases with the increase in R. The effect of thickness on propagation rate has also been

studied. A reduction in the crack propagation rates is observed with the reduction in specimen thickness.

7 ACKNOWLEDGEMENTS

The authors would like to acknowloage Aubert et Duval, in particular, M. André Grellier, for providing the testing material used in this investigation free of charge.

8 REFERENCES:

1. A. Persson, J. Bergström and C. Burman, 5th International Conference on Tooling, 1999, 167-177.
2. E. Ramous, A. Zambon, Proceedings of the 5th International conference on tooling, 1999, 179-184.
3. S. Hong and R. Weil, *Thin Solid Films.,* 283**,** 1996, 175.
4. R. Schwaiger and O. Kraft, *Scripta Materialia.*, 41(8), 1999, 823–829.
5. O. Kraft, R. Schwaiger and P. Wellner, *Mater Sci Eng.,* 2001, ,919.
6. S. Cravero and C. Ruggieri, *Engineering Fracture Mechanics.*, 74, 2007, 2735-2757.
7. M.S. Chiodo, S. Cravero, C. Ruggieri, Stress intensity factors for SE(T) specimens, Technical report, BT-PNV-68, Faculty of Engineering, University of Sao Paulo, 2006.
8. R. John and B. Rigling, *Engineering Fracture Mechanics.*, 60, 1998, 147-156.
9. P.C. Paris & F. Erdogan, *Journal of Basic Engineering.*, 85, 1963, 528-34.
10. D. Delagnes, Comportement et tenue en fatigue isotherme d'acier à outil Z 38 CDV 5 autour de la transition fatigue oligocyclique – endurance, PhD thesis, l'Ecole Nationale Supérieur des Mines de Paris., Work done at CROMeP EMAC Albi, 1998.
11. A. Oudin, Thermo-mechanical fatigue of hot work tools steels, PhD thesis, l'Ecole Nationale Supérieur des Mines de Paris., Work done at CROMeP EMAC Albi, 2001.